

Analysis of field emission projector patterns and issues of correct determination of local current characteristics of a multi-tip cathode

© A.G. Kolosko¹, E.O. Popov¹, S.V. Filippov¹, B.E. Mutygullin^{1,2}

¹ Ioffe Institute, St. Petersburg, Russia

² Peter the Great Saint-Petersburg Polytechnic University, St. Petersburg, Russia

E-mail: agkolosko@mail.ru

Received May 3, 2024

Revised September 27, 2024 Accepted October 30, 2024

A method for analyzing the structure of light responses in the glow patterns of a field projector has been developed. An algorithm for identifying areas corresponding to individual emission sites has been proposed. A theory of the occurrence of the halo effect, associated with the elastic rebound of electrons from the surface of the phosphor, has been confirmed.

Keywords: field emission, field emission projector, halo effect.

DOI: 10.61011/TPL.2024.12.60367.6598k

A field emission projector with a flat fluorescent screen is often used to analyze the properties of multi-tip field cathodes [1]. This system is occasionally referred to as IMLS (integral measurement system with the luminescent screen). It consists of a flat luminescent anode located close to a field cathode with the typical vacuum gap width measuring several hundred micrometers. Electron fluxes from individual emission sites form the so-called glow patterns on the screen, which are recorded by digital cameras. These patterns allow one to observe changes in the emission activity of individual sites, distribute the current load between them, and even calculate local emission characteristics suitable for theoretical analysis. The use of IMLS for evaluation of the uniformity of current load distribution and study of the characteristics of individual emitters within an array of other tips allows for targeted technological optimization of multi-tip field cathodes.

The blurring of emitter images in the glow pattern makes it impossible to determine unambiguously the areas corresponding to these emitters in order to, e.g., trace the operating characteristics of each emitter during field emission. The areas corresponding to individual emitters may be identified by setting a threshold brightness level [2]; the sizes of such areas necessarily increase with an increase in applied voltage, since the entire glow pattern becomes brighter in the process [3]. The relative size of these regions also allows one to estimate the fraction of emitters remaining stable over time and the proportion of emerging and deactivated emitters [4]. In particular, the overexposure effect (a natural limit on the brightness level in the digital camera sensor that records glow patterns) may be used to specify such a region. Horizontal plateaus will then be observed in the digitized profile of a glow pattern. The area of these plateaus may be taken as the emission area [5]. However, the relation between the area of the regions discussed above and the formal emission area, which is specified by theorists as the ratio of the total emitter current to the current density at its top, is ambiguous, as is the relation between the brightness profile of designated regions

and the local current characteristics of individual emitters. The issue is that the structure of light responses is affected by various parasitic effects [6].

The most natural of these effects is the dispersion of electrons in different directions along the cathode–anode path. The flux of electrons from the top of a carbon nanotube to the surface of a luminescent anode was simulated in [7]. It was demonstrated that the spot brightness profile has the form of a rounded peak with a near-parabolic shape.

Another effect often found in the glow patterns of quite different types of field cathodes is the emergence of a luminous halo around the central spot. The halo circles occasionally become discontinuous, assuming the shape of a ring. The observed halo effect was attributed in [8] to the rebound of a fraction of electrons from the site where they hit the anode (absolutely elastic reflection from the phosphor surface charged by electrons and return to the anode away from the initial site). Calculations have revealed that electron rebound distance Z may be written as

$$Z = 2d_{sep} \frac{\varepsilon_S}{eU}, \quad (1)$$

where d_{sep} is the electrode separation, ε_S is the energy of an electron rebounding from the surface, and U is the voltage between the cathode and the anode. Thus, the maximum rebound distance achieved at $\varepsilon_S = eU$ is $Z_{max} = 2d_{sep}$.

The dependence of halo radius on the electrode separation was demonstrated experimentally in the same study [8]: the radius increased linearly with separation. Notably, the halo size did not depend on the current strength (electron flux density).

We have already developed a method for analysis of glow patterns allowing one to determine the position of individual emitters and collect data on their emission properties under glow pattern flickering (real-time video processing) [9].

The aim of the present study is to analyze the structure of light responses in the glow pattern and develop a technique

for suppression of the influence of response overlap on the assessment of local properties of emitters.

The measurement setup was a vacuum system with a plane-parallel arrangement of electrodes in the measurement chamber fitted with a high-voltage source (high-voltage transformer) and a multi-channel computerized system for collecting, recording, and analyzing (in real time and in the signal emulation mode) data on field emission. The program for detection, recording, and processing of signals was written in the LabVIEW graphical programming language. A detailed description was provided in [9]. The vacuum level was no worse than 10^{-7} Torr. The electrode separation (from the cathode substrate to the anode) was $d_{A-C} = 570 \mu\text{m}$. The emission current level was $45 \mu\text{A}$. The glow patterns had a resolution of 1280×960 with $20 \mu\text{m}$ per pixel. A special program was written to analyze the structure of light responses in the glow pattern. This program performs three key operations: conversion of the glow pattern into a grayscale image with brightness level L_1 of a single pixel varying from 0 to 255, smoothing with a Fourier filter, and search for brightness peaks.

The test sample was an array of 20 silicon emitters in the form of octahedral pyramids with height $H \sim 200 \mu\text{m}$ and base width $W \sim 170 \mu\text{m}$ located at distance $D \sim 1000 \mu\text{m}$ from each other. The sample was fabricated at the National Research University of Electronic Technology by ultraviolet lithography as part of the project for development of X-ray facilities [10].

Light reflections observed in the glow patterns of pointed emitters may be divided into three groups: (1) luminous point; (2) luminous point with a round halo of an almost constant brightness; and (3) luminous point with an irregular-shaped halo.

Let's analyze the structure of light responses. The glow pattern analysis algorithm includes the following steps: (1) determination of the coordinates of brightness maxima (the position of emission sites in the glow pattern); (2) determination of the distance to the nearest neighbor for each site ($R_{\text{site-to-site}}$); (3) partitioning of the glow pattern around each site into concentric circles (with circle radius increment $\Delta R = 1$ px and the limit being $R_{\text{site-to-site}}$); (4) calculation of total brightness of all pixels in these circles $L_C = \sum_{\text{circle}} L_1$; (5) calculation of total brightness of pixels in the corresponding rings $L_R = \sum_{\text{ring}} L_1$; (6) calculation of average brightness of pixels in a ring $L_{RA} = L_R/A$, where A is the area of a ring with radius R measured in pixels (note that $A \sim R$, since the ring width is 1 px); and (7) reiteration of these calculations at different current levels I .

Figure 1, *a* presents the obtained dependences of L_C and L_R on radius R for the light response with a round halo (the plot is limited to a radius of 50 px where the brightness drops to zero).

The $L_R(R)$ dependence has a characteristic peak at the start of the range (denoted with an arrow in Fig. 1, *a*), which indicates the onset of reduction in brightness of the light response.

The circle with radius R_0 corresponding to the onset of reduction of the total brightness in the ring may be regarded

as a projection of the emission surface of an individual emitter on the glow pattern, and its area may be called the „area of light response of the emitting surface.“ The next significant peak in this dependence corresponds to the onset of reduction in brightness of the halo (R_1 from 25 to 35 px).

Figure 1, *b* shows the $L_R(R)$ dependences for 19 emission sites in the multi-tip cathode. It turned out that all of them had the same emission region radius $R_0 = 6$ px, which is indicative of a similarity in shape (radius of curvature) of their tips. Moreover, the radii of halos (sites with halos — red, brown, and black curves) also turned out to be close to each other: $R_1 \sim 30$ px.

Figure 2, *a* shows the brightness profile of the response with a halo (see the inset in Fig. 1, *a*): the dependence of average brightness in the ring $L_{RA}(R)$. The profile of the same site obtained by recording brightness L_P of individual pixels along horizontal and vertical lines passing through the maximum is presented in the inset. It is evident that the dependences presented in Fig. 2, *a* and its inset are of the same nature; however, the analysis with brightness averaging in the rings yields a smoother dependence (as a ratio of two plots $L_R(R)$ and $A(R)$; see the lower inset in Fig. 1, *a*).

The shape of the peak in Fig. 2, *a* corresponds to the one obtained in [7] and is close to a parabolic dependence. Its distinguishing feature is the presence of a halo in the form of a horizontal shoulder with almost uniform brightness and radius $R_{\text{halo}} \sim 45$ px. If we subtract the radius of the central spot from the halo radius, the maximum rebound is obtained: $Z_{\text{max}} = R_{\text{halo}} - R_0 = 39$ px = $780 \mu\text{m}$. The separation between the emitter tips and the anode is $d_{\text{sep}} = d_{A-C} - H \approx 370 \mu\text{m}$. Thus, distance $2d_{\text{sep}} = 740 \mu\text{m}$ is indeed close to maximum rebound distance.

Figure 2, *b* shows the $L_{RA}(R)$ dependences for emission sites found in the glow pattern of the array of emitters. The refinement of brightness peaks and their sorting revealed that halos form around the most active (bright) emitters. This may be attributed to the fact that the phosphor has a glow limit, and insufficiently high emission current densities may induce no visible luminescence in this region. The brightest site has another nearby maximum that is not resolved by the program; this makes the dependence (red curve) in the halo area gently sloping rather than horizontal. Owing to the overlap of two responses (orange and brown curves), the center of the response with no halo is brighter than the center of the response with a halo. This overlap is also behind the fact that the brightness profile of responses without halos does not drop to zero at high R (blue and crimson curves). Note that the brightness profiles of responses having no overlap with the halos of neighbors are approximated fairly well by a Gaussian curve.

Thus, the reflection structure may be characterized by a sum of three functions

$$L(R) = f_{\text{Gauss}}(R) + f_{\text{halo}}(R) + f_{\text{overlap}}(R), \quad (2)$$

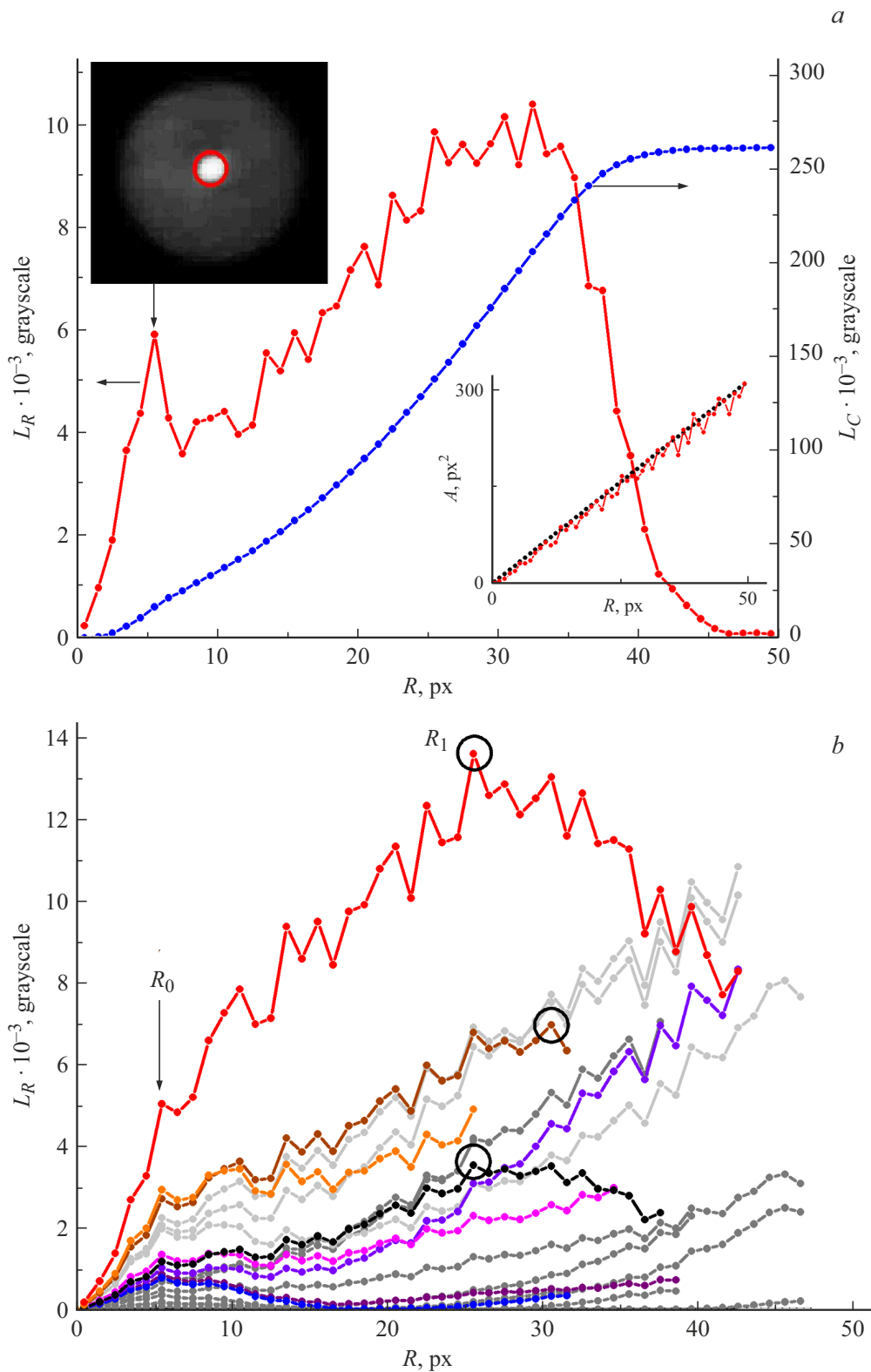


Figure 1. Dependence of the total brightness in the circle and in the ring of light response on distance R to the emission site. *a* — L_C and L_R values for an individual emission site with a halo. The upper inset shows the light response, while the lower one presents the dependences of ring area A on its radius R : the ideal dependence (black dots) and the one calculated by pixels (red curve). *b* — L_R values for 19 emission sites in the array with partially overlapping light responses in the glow pattern. A color version of the figure is provided in the online version of the paper.

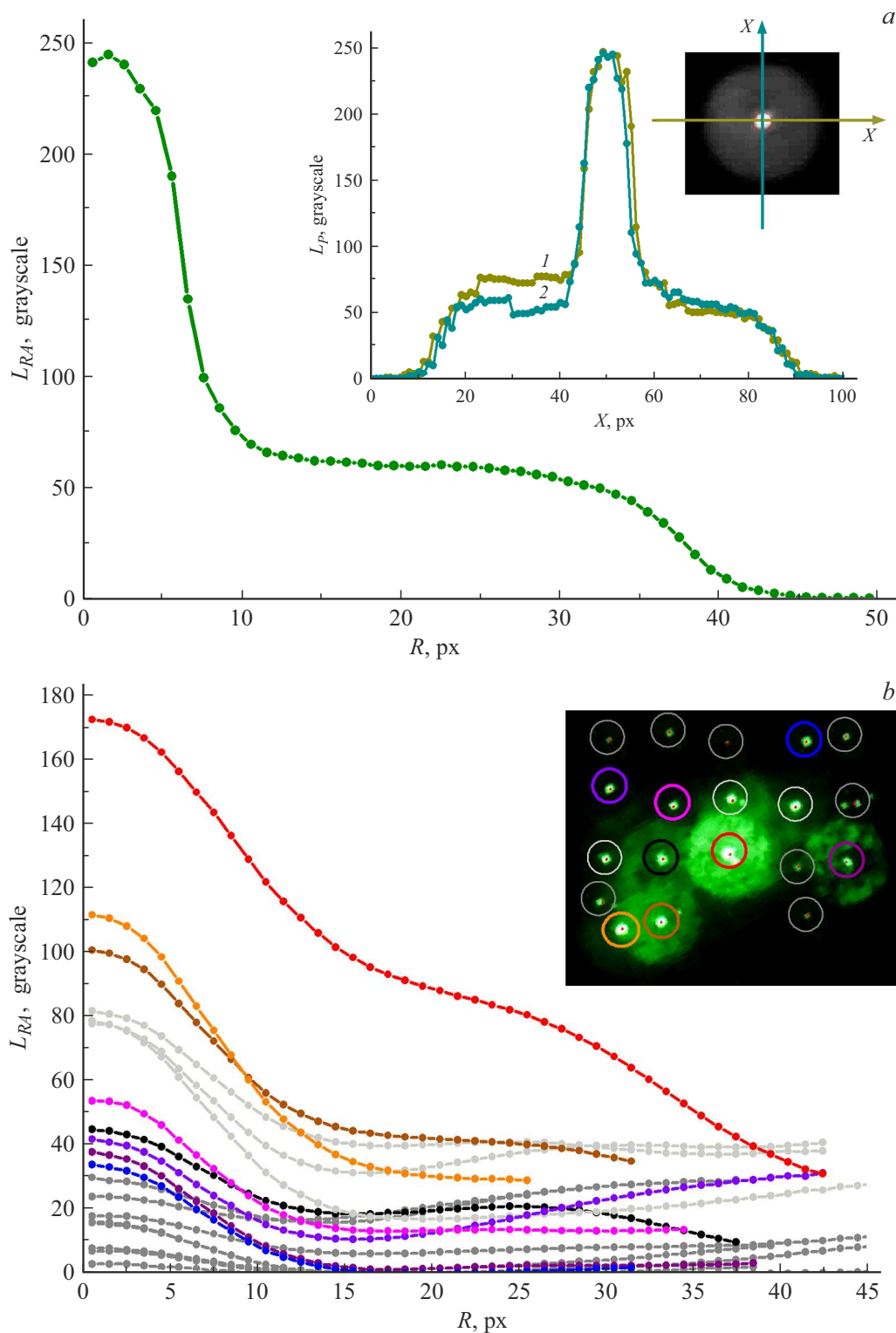


Figure 2. Brightness profiles of light responses (dependences of the L_{RA} value). *a* — Response with a halo. Pixel brightness profile L_P along horizontal (1) and vertical (2) lines is shown in the inset. *b* — Dependences for all 19 responses. The inset presents a glow pattern with emission sites indicated by circles matching in color with the corresponding curve in the main part of the figure. A color version of the figure is provided in the online version of the paper.

where function $f_{Gauss}(R)$ has an inflection in the region of radius R_0 and represents the direct response

of an electron flux at the phosphor, function $f_{halo}(R)$ has the form of a constant addition limited by radius

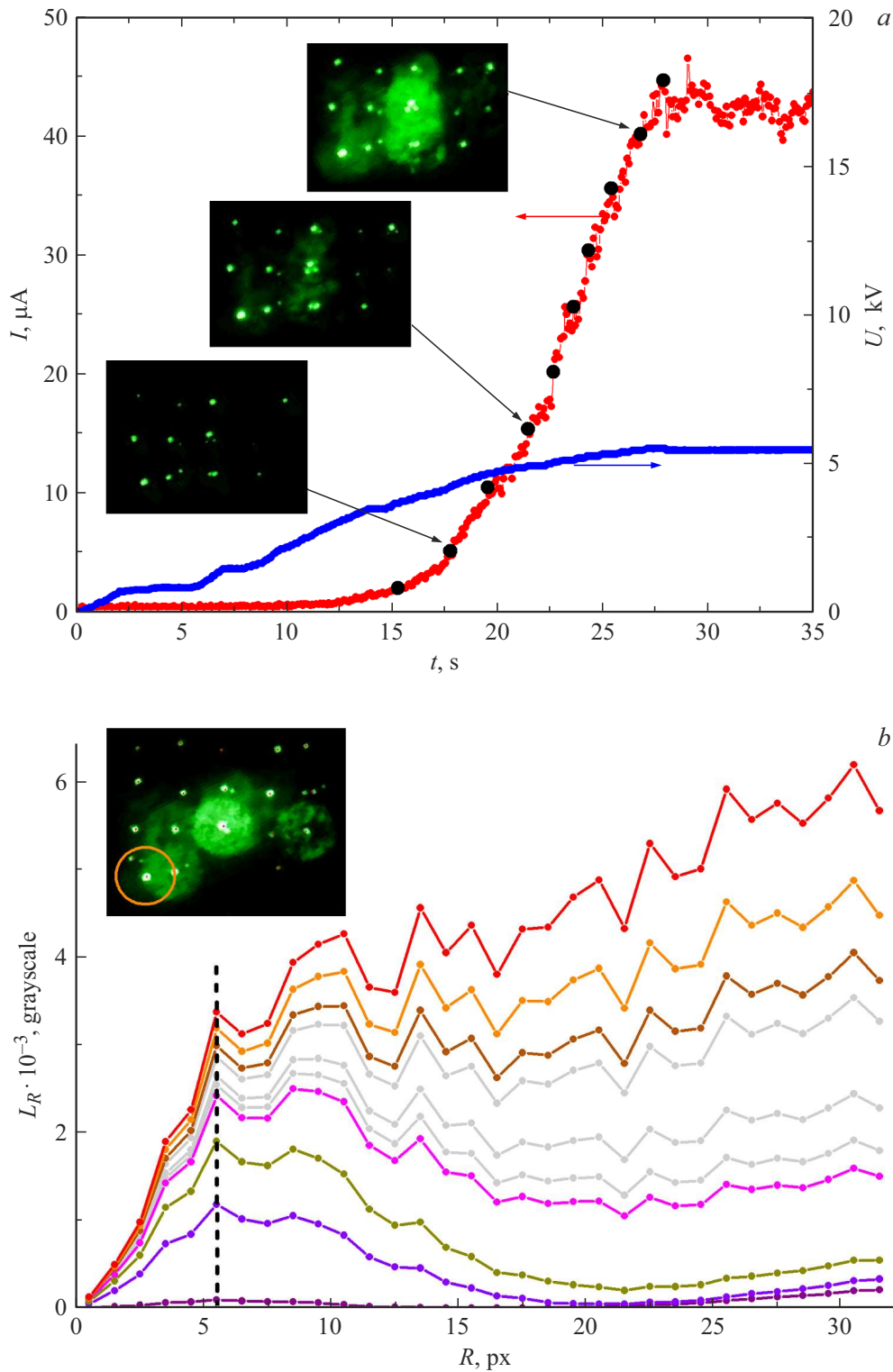


Figure 3. Variation of brightness of the glow pattern. *a* — Time dependences of the emission current and voltage levels. The insets show the glow patterns recorded at time points indicated by the arrows. *b* — Variation of the radius dependence of the total ring brightness with a change in current (the curves correspond to dots in panel *a*, and the vertical dashed line indicates the stability of radius R_0) for a single emission site shown in the inset.

$R_{halo} \sim 4d_{sep}$, and function $f_{overlap}(R)$ is responsible for the effect of overlap of halos of neighboring responses

(parasitic illumination) and also has the form of a constant addition.

Figure 3,*a* shows the variation of voltage applied to the sample and the corresponding emission current (with a step of $\sim 5\mu\text{A}$). Changes in the glow pattern induced by an increase in current are illustrated in the insets. At low currents, the light responses of emitters are easy to distinguish and do not overlap. At currents above $15\mu\text{A}$, halos start to emerge around the brightest points and enhance the brightness of neighboring responses. The parasitic increase in brightness of certain responses leads to an increase in local currents distributed to them and to a reduction in local currents received by isolated responses.

The analysis of all recorded glow patterns revealed that the sizes of both the emission area of responses (R_0) and the halos do not change with a reduction in voltage: the central spot and the halo simply grow dimmer, eventually falling completely out of the detection range.

Figure 3,*b* shows the variation of the profile of a single light response (dependence of the total brightness of pixels in a ring on ring radius $L_R(R)$) with a change in current. The vertical dashed line indicates the stability of radius R_0 (the position of the first peak). Owing to the mutual overlap of responses, the halo profile (points with $R > R_0$) assumes a shape differing from the profile of an individual response (Fig. 1,*a*) and varies profoundly with increasing current.

Conflict of interest

The authors declare that they have no conflict of interest.

References

- [1] N.V. Egorov, E.P. Sheshin, *Field emission electronics*. Springer Ser. in Advanced Microelectronics (Springer, Cham, 2017), vol. 60. DOI: 10.1007/978-3-319-56561-3
- [2] A.S. Chepusov, *Svoistva avtoemissionnykh katodov iz uglerodnykh materialov v usloviyakh tekhnicheskogo vakuuma*, Candidate's Dissertation in Engineering (Inst. Elektrofiz. Ural. Otd. Ross. Akad. Nauk, Ekaterinburg, 2018) (in Russian).
<https://elar.urfu.ru/bitstream/10995/72406/1/urfu2010.d.pdf>
- [3] R. Patra, A. Singh, V.D. Vankar, S. Ghosh, *Adv. Mater. Lett.*, **7** (10), 771 (2016). DOI: 10.5185/amlett.2016.6368
- [4] Y. Shiratori, K. Furuichi, S. Noda, H. Sugime, Y. Tsuji, Z. Zhang, Y. Yamaguchi, *Jpn. J. Appl. Phys.*, **47** (6R), 4780 (2008). DOI: 10.1143/JJAP.47.4780
- [5] D. Lysenkov, H. Abbas, G. Müller, J. Engstler, K.P. Budna, J.J. Schneider, *J. Vac. Sci. Technol. B*, **23** (2), 809 (2005). DOI: 10.1116/1.1868696
- [6] A.G. Kolosko, S.V. Filippov, E.O. Popov, *St. Petersburg Polytech. Univ. J. — Physics and Mathematics*, **16** (1.2), 39 (2023). DOI: 10.18721/JPM.161.205
- [7] M. Marchand, C. Journet, C. Adessi, S.T. Purcell, *Phys. Rev. B*, **80** (24), 245425 (2009). DOI: 10.1103/PhysRevB.80.245425
- [8] K.N. Nikolski, A.S. Baturin, A.I. Knyazev, R.G. Tchesov, E.P. Sheshin, *Tech. Phys.*, **49** (2), 250 (2004). DOI: 10.1134/1.1648964
- [9] E.O. Popov, A.G. Kolosko, S.V. Filippov, E.I. Terukov, R.M. Ryazanov, E.P. Kitsyuk, *J. Vac. Sci. Technol. B*, **38** (4), 043203 (2020). DOI: 10.1116/6.0000072
- [10] N.A. Djuzhev, G.D. Demin, N.A. Filippov, I.D. Evsikov, P.Yu. Glagolev, M.A. Makhboroda, N.I. Chkhalo, N.N. Salashchenko, S.V. Filippov, A.G. Kolosko, E.O. Popov, V.A. Bespalov, *Tech. Phys.*, **64** (12), 1742 (2019). DOI: 10.1134/S1063784219120053.

Translated by D.Safin